sciendo

DOI: 10.2478/ata-2022-0020

Acta Technologica Agriculturae 3/2022 *Volodymyr Bulgakov et al.*

Acta Technologica Agriculturae 3
Nitra, Slovaca Universitas Agriculturae Nitriae, 2022, pp. 131–136

A STUDY OF DYNAMIC LOADS OF A FLEXIBLE SECTIONAL SCREW CONVEYOR

Volodymyr BULGAKOV[1], Oleksandra TROKHANIAK[1], Valerii ADAMCHUK[2], Mykhailo CHERNOVOL[3], Maroš KORENKO[4], Ilmars DUKULIS[5], Semjons IVANOVS[5]*

[1]National University of Life and Environmental Sciences of Ukraine, Ukraine
[2]Institute of Mechanics and Automation of Agricultural Production of the National Academy of Agrarian Sciences of Ukraine, Ukraine
[3]Central Ukrainian National Technical University, Ukraine
[4]Slovak University of Agriculture in Nitra, Slovakia
[5]Latvia University of Life Sciences and Technologies, Latvia

When using complex spatial patterns for transportation, the straight screw conveyors have a series of obvious disadvantages. This paper presents a design of a flexible screw sectional working body that allows increasing the functional and operational characteristics of screw conveyors used in the transportation of bulk agricultural materials. A mathematical model of the dynamic system of a flexible screw conveyor has been established, and dynamic starting torques have been calculated at the rated load of loaded screw, and when the system is braking. Analysis of the results obtained shows that, with significant damping coefficients, the start-up transition process occurs smoothly, and the load reaches its rated value without torque and speed fluctuations. It has been established that fast braking significantly increases the dynamic loads that may exceed the maximum critical torque of the electric motor (by 50–70% on average) and the rated load torque (by 2.5–3 times).

Keywords: transportation; bulk material; flexible screw conveyor; model

Transportation of bulk agricultural materials in closed technological trunks is one of the main ways of their transfer in the production processes (Mondal and Ghosh, 2018; Lech, 2001).

There are known various technological systems for transportation of agricultural materials, and they have both advantages and disadvantages. Several investigations (Yao et al., 2014; Tian et al., 2018; Loveikin and Rogatynska, 2011; Qi et al., 2017) have been devoted to the issue of determining more advanced technical solutions. In agricultural practice, the screw conveyors have long been widely used to transport various kinds of bulk agricultural materials (grain, granulated seeds, bran, animal feed, mineral fertiliser granules, etc.). However, when using complex spatial patterns for transportation, the straight screw conveyors have a series of obvious disadvantages (Hevko et al., 2016; Roberts, 2015). High mobility of loading and unloading technological processes with a minimum degree of damage to the material on curved routes can be ensured by utilization of flexible screw conveyors. However, the existing flexible screw working bodies have a number of disadvantages and cannot fully satisfy the operational requirements for such types of conveyors (Hevko et al., 2019; Hevko et al., 2012; Lech, 2001; Rohatynskyi et al., 2016; Owen and Cleary, 2010.). Employment of shaftless flexible spirals of augers leads to their rapid deterioration when conveyors operate on curved routes due to the occurrence of alternating cyclic loads. Implementation of the working body in a form of solid or sectional shaft, on which individual elements of helical ribs are located, leads to an essential complication of the technological body design, an increase in its material consumption, which entails an increase in the energy consumption and ultimately damage to the transported materials (Lyashuk et al., 2015; Hevko et al., 2017; Pankiv and Tokarchuk, 2017), as well as other shortcomings. The problem of studying the work process and improving the flexible screw conveyors is relevant and requires further research for more optimal solutions.

The purpose of this study is to develop a mathematical model of the dynamic system of a flexible screw conveyor for calculating the dynamic starting torques, and to study its functional and operational characteristics in order to justify the optimal parameters.

Material and methods

In a process of searching for more optimal technical solutions, an experimental design of a flexible sectional screw working body was used (Fig. 1) (UA 85011, 2013). It was implemented in a form of two identical adjacent spirals – the left one [1] and the right one [2] – the ends of which were rigidly connected with their internal diameters to separate splined bushings [3]. In the internal diameters of bushings [3] were semi-circular axial splines [4] that were evenly spaced around the circumference and in interaction with cylindrical hinges [5] through balls [6], which were rolled in sockets [7] at the ends of cylindrical hinges with

Contact address: Semjons Ivanovs, Latvia University of Life Sciences and Technologies, Latvia, e-mail: semjons@apollo.lv

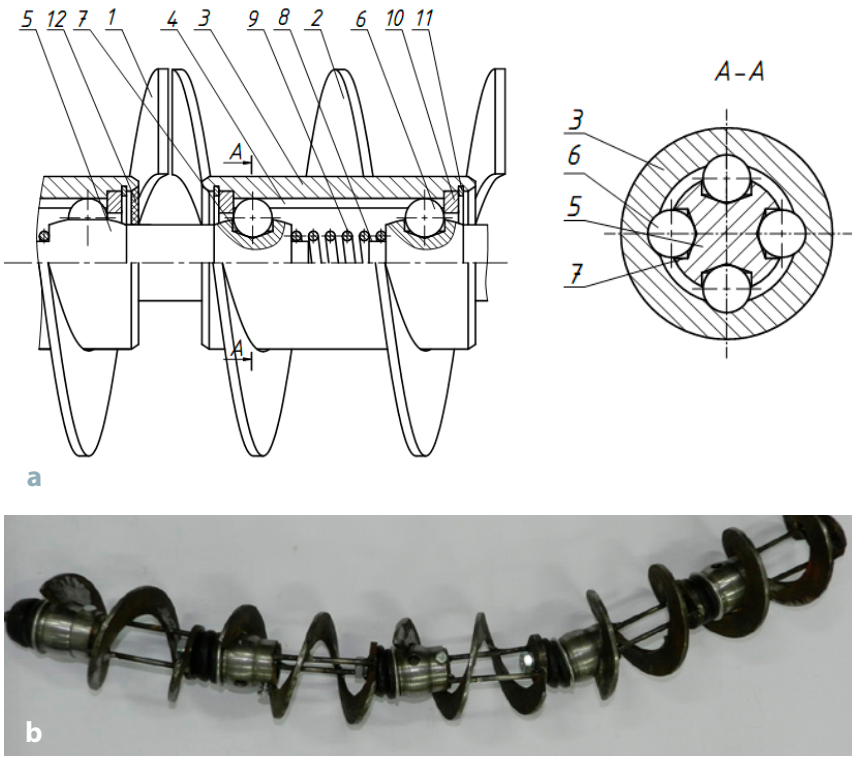


Fig. 1 Scheme (a) and general view (b) of the flexible screw sectional working body

the possibility of free twisting such as a cardan gear. However, the ends of the cylindrical hinges [5] of a smaller diameter [8] were in interaction with the inner diameters of the expansion springs [9]. Additionally, the balls [6] at the ends of cylindrical hinges [4] were in interaction with the restrictive rings [10], which were at the edges of sections in interaction with the retaining rings [11]. If necessary, to protect the internal holes of the splined bushings [3] from two ends, they were closed with sleeves [12]. The screw working body work can be described as follows. During the spiral section rotation [1], the rotational movement is transmitted through the rolling elements [6] to the cylindrical hinges [5] and adjacent sections of the working screw body. The advantages of proposed flexible screw working body include an increase in the loading capacity and expansion of technological capabilities. In order to estimate the maximum loads that develop in the elements of the flexible screw conveyor during the transitional starting and braking processes, its dynamic model was created, and a resulting solution was analysed. Furthermore, to simplify the model construction and its perception, a liberty of idealisation was taken and the presence and impacts of the gearbox from the electric motor to the shaft (i.e., it was conditionally assumed that the gear ratio was equal to one) were not taken into account. The gear ratio certainly affects the torque value, yet the nature of the relative impact of the damping coefficients on the change in the torque, which is of interest to this paper, is affected only slightly.

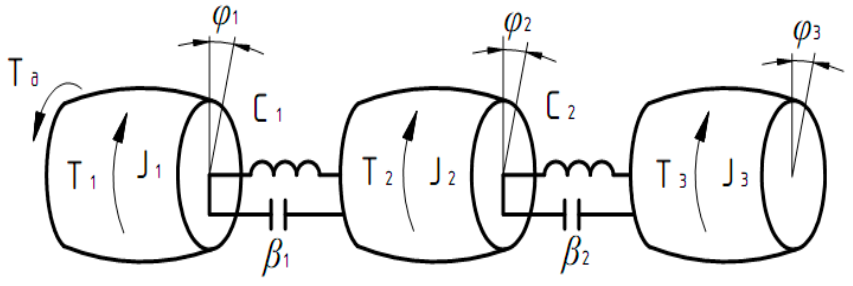


Fig. 2 Scheme of the dynamic model

A simplified dynamic model as an elastic three-mass rotating system, which is subjected to external torques from the electric motor and the transported material, is provided in Fig. 2.

The first rotating mass J_1 represents the total mass of the drive mechanism (the motor, gearbox and clutch). It is affected by the torque of the electromagnetic forces of the electric motor T_d, reduced to the axis of rotation of the screw, and the efforts of the friction forces T_1 in the drive mechanism. The second rotating mass J_2 is a combined mass of the first section of the flexible screw conveyor together with the mass of the transported material. It is affected by the moment of resistance, which can be represented as the sum of two components – the steady moment of dry friction T_2 and the moment of viscous friction, which depends on the speed of movement. In a similar way, J_3 corresponds to the summary mass of the next section of the flexible screw conveyor. Obviously, if there are several sections of the conveyor, the number of rotating masses must correspond to their number. However, in models investigating the transient processes, due to the presence of significant friction forces of the bulk material leading to damping of the oscillations of following sections, it is possible to replace a long chain of sections with a summary torque moment of resistance T_3, which is applied to the section with mass J_3. This is also true for as a certain moment of viscous friction. This assumption significantly reduces the complexity of the system analysis, without affecting the determination of the maximum dynamic loads that arise in the drive mechanism and the first section of the conveyor. Therefore, the study is confined to a dynamic system consisting of three characteristic rotating masses. Each section is connected to the next elastic element, the total rigidity of which is determined by the elastic properties of the screw section and the hinge mechanism. The dynamic model (Fig. 2) can be described by a system of three differential equations of movement

(Eq. 1). Each equation describes the movement of the corresponding rotating mass:

$$\left.\begin{aligned} J_1\ddot{\varphi}_1 &= T_d - c_1(\varphi_1-\varphi_2) - \beta_1\dot{\varphi}_1 - T_1\,\mathrm{sgn}(\dot{\varphi}_1) \\ J_2\ddot{\varphi}_2 &= c_1(\varphi_1-\varphi_2) - c_2(\varphi_2-\varphi_3) - \beta_2\dot{\varphi}_2 - T_2\,\mathrm{sgn}(\dot{\varphi}_2) \\ J_3\ddot{\varphi}_3 &= c_2(\varphi_2-\varphi_3) - \beta_3\dot{\varphi}_3 - T_3\,\mathrm{sgn}(\dot{\varphi}_3) \end{aligned}\right\} \quad (1)$$

where: φ_1, φ_2, φ_3 – rotation angles of the rotating masses J_1, J_2, J_3, respectively; c_1, c_2, c_3 – stiffness of the connecting elements; β_1, β_2, β_3 – coefficients of the viscous damping forces acting on the corresponding masses

The electric motor torque can be described by its mechanical characteristic, which relates the rotation speed and the torque. The simplest static mechanical characteristic of the electric motor does not take into account electromagnetic processes in the motor. As a driving motor, an asynchronous electric motor with a squirrel-cage rotor is most frequently used without a starting current and a speed control circuit, i.e., the motor is included in the direction network. In this case, its mechanical characteristic can be written as:

$$T_d = \frac{2T_k}{\frac{s}{s_k} + \frac{s_k}{s}} \quad (2)$$

The values in Eq. 2 are determined by the formulas:

$s_k = \frac{\omega_0 - \omega_k}{\omega_0}$ – critical slip of the electric motor,

$s = \frac{\omega_0 - \dot{\varphi}_1}{\omega_0}$ – running slipping of the electric motor,

where: ω_0 – synchronous frequency of rotation of the electric motor rotor; ω_k – critical frequency of rotation of the electric motor rotor; T_k – critical torque of electric motor

The last three values were determined by the tabular parameters of the electric motor and had to be reduced to the screw rotation axis.

The system of differential equations (Eq. 1) is non-linear; therefore, its analytical solution is difficult. In connection to it, a numerical method was applied based on the transformation of a system of the second-order differential equations into a system of the first-order differential equations with twice as many of them (Derevjanko et al; 2020; Bulgakov et al., 2019). To do this, corresponding substitutions were performed.

$$\left.\begin{aligned} \varphi_1 &= u \\ \dot{u} &= \frac{T_d - c_1(\varphi_1-\varphi_2) - \beta_1\dot{\varphi}_1 - T_1\,\mathrm{sgn}(\dot{\varphi}_1)}{J_1} \\ \varphi_2 &= v \\ \dot{v} &= \frac{c_1(\varphi_1-\varphi_2) - c_2(\varphi_2-\varphi_3) - \beta_2\dot{\varphi}_2 - T_2\,\mathrm{sgn}(\dot{\varphi}_2)}{J_2} \\ \varphi_3 &= w \\ \dot{w} &= \frac{c_2(\varphi_2-\varphi_3) - \beta_3\dot{\varphi}_3 - T_3\,\mathrm{sgn}(\dot{\varphi}_3)}{J_3} \end{aligned}\right\} \quad (3)$$

To solve the system (Eq. 3), it is advisable to apply the Runge-Kutta numerical method, which has proven itself convenient and reliable for solving systems of equations that describe dynamic models of oscillating mechanical systems (Butcher, 2008; Hairer et al., 2006). At the start, the system of masses beginning the movement was at rest, therefore, the initial conditions were as follows:

$$\left.\begin{aligned} \varphi_1(0) &= 0 \\ \varphi_2(0) &= 0 \\ \varphi_3(0) &= 0 \\ u(0) &= \dot{\varphi}_1(0) = 0 \end{aligned}\right\} \quad (4)$$

Table 1 Numerical values of the mass, the force and the elastic coefficients

Name of the value	Designation	Numerical value	Unit of measurement
Rotating mass of the drive	J_1	2	kg·m^2
Rotating mass of the 1st section of the screw	J_2	0.01	kg·m^2
Rotating mass of the 2nd section of the screw	J_3	0.01	kg·m^2
Rigidity of the drive	c_1	2000	N·m
Rigidity of the elements of the 1st section	c_2	1000	N·m
Coefficient of viscous friction of the mass of the drive	β_1	0.5	N·m·s
Coefficient of viscous friction of the 1st section	β_2	5	N·m·s
Coefficient of viscous friction of the 2nd section	β_3	5	N·m·s
Moment of resistance of the drive elements	T_1	10	N·m
Moment of resistance of the 1st section	T_2	20	N·m
Moment of resistance of the 2nd section	T_3	200	N·m
Rated frequency of rotation of the drive	ω_0	10	s^{-1}
Critical slipping	s_k	0.25	–
Critical torque	T_k	500	N·m

$$\left.\begin{aligned} v(0) &= \dot{\varphi}_2(0) = 0 \\ w(0) &= \dot{\varphi}_3(0) = 0 \end{aligned}\right\} \quad (4)$$

In order to analyse the influence of certain system parameters on the magnitude of dynamic loads during the start-up period, the force and the elastic coefficients were calculated by assuming the following numerical values of the mass given in Table 1.

The values of friction moments and the critical moment were selected for the calculated rated power of the electric motor of 2.2 kW. In order to increase the starting torque, which is required when starting the screw conveyor under load, an asynchronous motor with increased slip was selected. The second, especially stressed case of the movement of the flexible screw conveyor, is sudden braking due to jamming of material or accidental entry of a certain object into the conveying zone. At this moment, the system rotating at a constant speed begins to brake, increasing the braking torque until the drive stops completely. Mathematically, by applying certain assumptions, this can be written as a linear increase in torque T_3 in time t from the initial value T_{30} to the maximum when the movement of the rotating mass J_3 is stopped:

$$T_3 = T_{30} + Mt \quad (5)$$

where: M – factor of the braking torque growth

The value M determines the braking speed of the drive. In real systems, the deceleration time can last from 0.1 s to 5 s. A short time is typical for incompressible bulk materials (sand, dry grain materials), but a long deceleration time is typical for the transportation of compressible media (soft grain materials, animal feed, seeds, chaff).

The conveyor movement during braking can be divided into 2 stages. The first is braking until the rotating mass J_3 stops. At this movement stage, the system can be described by the same equations (Eqs 1–3), yet with different initial conditions that correspond to the final values of the angles and their velocities in a steady movement before the start of braking at time t_1, but the braking torque is determined based on Eq. 5:

$$\left.\begin{aligned} \varphi_1(0) &= \varphi_1(t_1) \\ \varphi_2(0) &= \varphi_2(t_1) \\ \varphi_3(0) &= \varphi_3(t_1) \\ u(0) &= \dot{\varphi}_1(t_1) = \omega_1 \\ v(0) &= \dot{\varphi}_2(t_1) = \omega_1 \\ w(0) &= \dot{\varphi}_3(t_1) = \omega_1 \end{aligned}\right\} \quad (6)$$

The second stage of movement includes fluctuations of masses J_1 and J_2, connected through the elastic elements c_1 and c_2 to the stopped mass J_3. At the second stage, the elastic system is described by a system of two differential equations:

$$\left.\begin{aligned} J_1\ddot{\varphi}_1 &= T_d - c_1(\varphi_1 - \varphi_2) - \beta_1\dot{\varphi}_1 - T_1\,\mathrm{sgn}(\dot{\varphi}_1) \\ J_2\ddot{\varphi}_2 &= c_1(\varphi_1 - \varphi_2) - c_2(\varphi_2 - \varphi_3) - \beta_2\dot{\varphi}_2 - T_2\,\mathrm{sgn}(\dot{\varphi}_2) \end{aligned}\right\} \quad (7)$$

Accordingly, after replacement, it is possible to obtain a system of four first-order differential equations:

$$\left.\begin{aligned} \dot{\varphi}_1 &= u \\ \dot{u} &= \frac{T_d - c_1(\varphi_1 - \varphi_2) - \beta_1\dot{\varphi}_1 - T_1\,\mathrm{sgn}(\dot{\varphi}_1)}{J_1} \\ \dot{\varphi}_2 &= v \\ \dot{v} &= \frac{c_1(\varphi_1 - \varphi_2) - c_2(\varphi_2 - \varphi_3) - \beta_2\dot{\varphi}_2 - T_2\,\mathrm{sgn}(\dot{\varphi}_2)}{J_2} \end{aligned}\right\} \quad (8)$$

with the corresponding initial conditions, which are final for the moment of time t_2 of stopping mass J_3:

$$\left.\begin{aligned} \varphi_1(0) &= \varphi_1(t_2) \\ \varphi_2(0) &= \varphi_2(t_2) \\ u(0) &= \dot{\varphi}_1(t_2) = \omega_2 \\ v(0) &= \dot{\varphi}_2(t_2) = \omega_2 \end{aligned}\right\} \quad (9)$$

Consequently, a mathematical model of the dynamic system of flexible screw conveyor was obtained, the dynamic starting torques were calculated at the rated load of the loaded screw and during system braking.

Results and discussion

Based on the created mathematical model of flexible screw conveyor dynamic system, the dynamic starting torques were calculated at the rated load of loaded screw. The results of calculations are presented in Figs 3–6. The graphical results of dynamic loads during system braking (Eqs 5–9) are shown in Figs 7–10.

Analysis of the obtained results proved that, with significant damping coefficients, the start-up transition process occurs smoothly, and the load reaches its rated value without torque and speed fluctuations. At low damping, a certain transient oscillatory process was observed; however, the dynamic loads did not exceed 20% of the rated value. There were considered cases of slow and fast braking. Analysis of the graphs showed that fast braking significantly increases the dynamic loads, which can exceed the

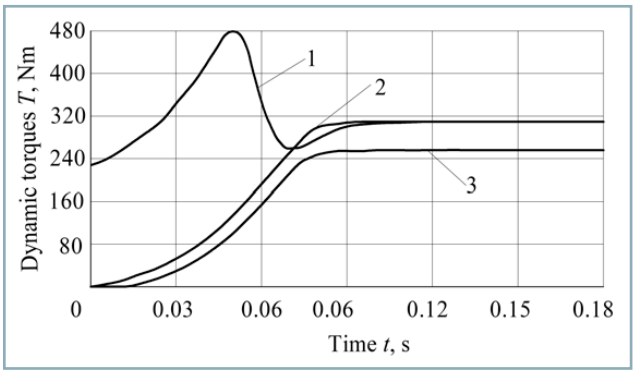


Fig. 3 Changes in the dynamic torques of the drive and the conveyor elastic sections with significant external damping $\beta_1 = \beta_3 = 5$: 1 – T_d; 2 – $c_1(\varphi_1 - \varphi_2)$; 3 – $c_2(\varphi_2 - \varphi_3)$

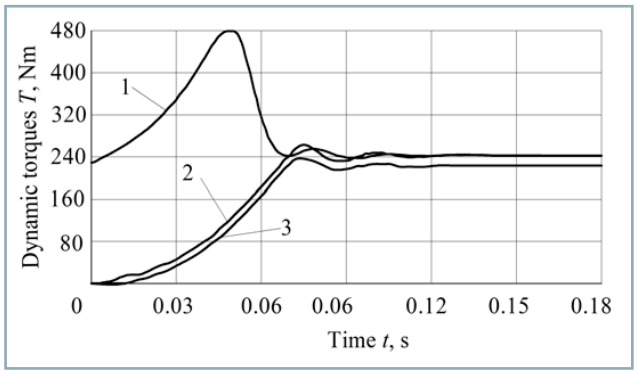


Fig. 4 Changes in the dynamic torques of the drive and the elastic conveyor sections with small external damping $\beta_2 = \beta_3 = 1$: 1 – T_d; 2 – c_1 ($\varphi_1 - \varphi_2$); 3 – c_2 ($\varphi_2 - \varphi_3$)

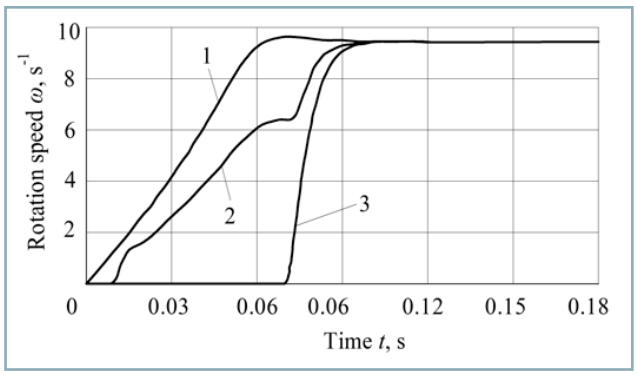


Fig. 5 Rotation speeds of masses with significant external damping $\beta_2 = \beta_3 = 5$: 1 – ω_1; 2 – ω_2; 3 – ω_3

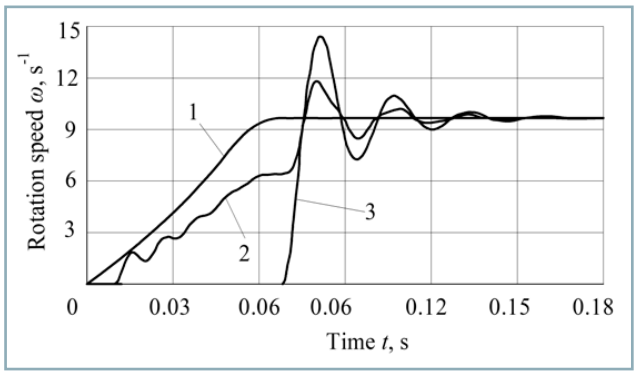


Fig. 6 Rotation speeds of masses with small external damping $\beta_2 = \beta_3 = 1$: 1 – ω_1; 2 – ω_2; 3 – ω_3

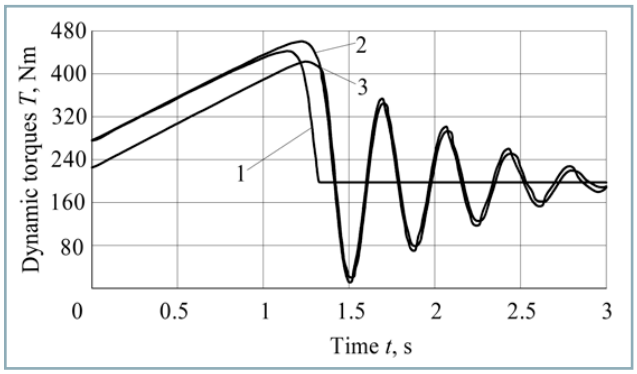


Fig. 7 Dynamic torques in the conveyor sections during slow braking (1 s): 1 – T_d; 2 – c_1 ($\varphi_1 - \varphi_2$); 3 – c_2 ($\varphi_2 - \varphi_3$)

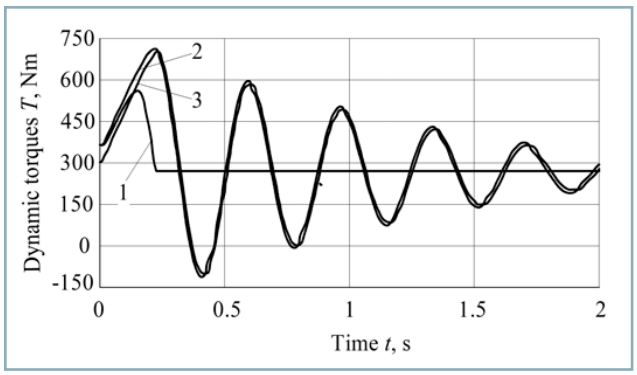


Fig. 8 Dynamic torques in the conveyor sections during fast braking (0.2 s): 1 – T_d; 2 – c_1 ($\varphi_1 - \varphi_2$); 3 – c_2 ($\varphi_2 - \varphi_3$)

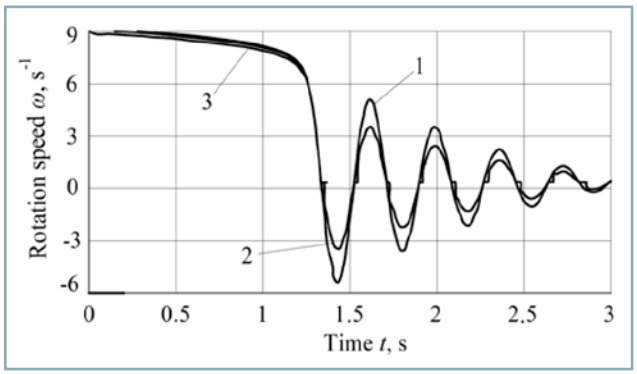


Fig. 9 Speeds of the conveyor sections during slow braking: 1 – ω_1; 2 – ω_2; 3 – ω_3

maximum critical torque of the electric motor (by 50–70% on average) and the rated load torque (by 2.5–3 times). To ensure the strength of screw sections during braking, it is necessary to provide the safety elements (couplings) with a response torque of less than 1.5 times the rated response torque. These results correlate with observations of Hevko et al. (2012) and Loveikin and Rogatinska (2011). Analysis showed that the dynamic loads are critical during jamming when they essentially exceed the allowed values, not during the system start-up.

In addition to theoretical research, carried out to determine the influence of transportation parameters of a granular medium and the conveyor design parameters on the torque, a full-factor experiment was carried out, i.e., the torque dependence on changes in three main factors was determined: screw rotation frequency, material lifting height and bending radius of the hinged connection of flexible screw sectional working body. A detailed presentation of this experiment and its results will be reflected in our subsequent publication.

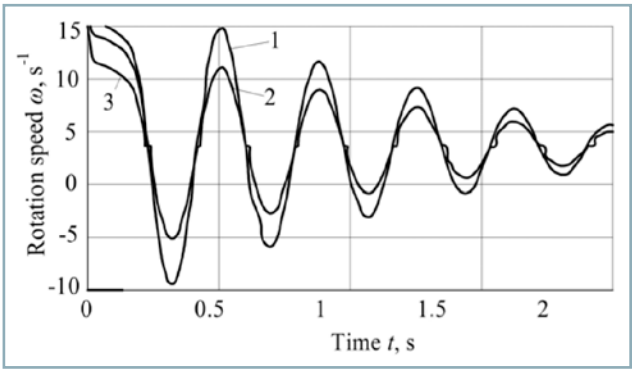


Fig. 10 Speeds of the conveyor sections during fast braking (0.2 s): 1 – ω_1; 2 – ω_2; 3 – ω_3

Conclusion

Utilization of developed flexible screw sectional working body allows expansion of functional possibilities and improvement of performance characteristics of the screw conveyors. On the basis of created mathematical model of the dynamic system of flexible screw conveyor, the dynamic starting torques were calculated at the rated load of loaded screw. Analysis of the results obtained showed that, with significant damping coefficients, the start-up transition process occurs smoothly, and the load reaches its rated value without torque and speed fluctuations. At low damping, a certain transient oscillatory process was observed; however, the dynamic loads did not exceed 20% of the rated value.

Results analysis from calculating of dynamic loads during the system braking indicates that fast braking significantly increases the dynamic loads, which can exceed the maximum critical torque of the electric motor (by 50–70% on average) and the rated load torque (by 2.5–3 times). To ensure the strength of screw sections during braking, it is necessary to provide safety elements (couplings) with a response torque of less than 1.5 times the nominal response torque.

References

BULGAKOV, V. – IVANOVS, S. – SAFCHENKO, I. – BORIS, A. – RYCHLIVSKYJ, P. 2019. Theoretical research of the design and technological parameters of a device for lifting of deep-seated table root crops. In Acta Technologica Agriculturae, vol. 22, no. 3, pp. 99–103.

BUTCHER, J. 2008. Numerical Methods for Ordinary Differential Equations. New York : John Wiley & Sons, 544 pp. ISBN 9780470723357.

DEREVJANKO, D. – HOLOVACH, I. – BULGAKOV, V. – IHNATIEV Y. – NOZDROVICKÝ, L. 2020. Mathematical model of uniform cereal crops seeding using a double-disk coulter. In Acta Technologica Agriculturae, vol. 23, no. 4, pp. 195–200.

HAIRER, E. – LUBICH, C. – WANNER, G. 2006. Geometric Numerical Integration: Structure-Preserving Algorithms for Ordinary Differential Equations. (2nd ed.), New York : Springer-Verlag, 660 pp. ISBN 9783540306634.

HEVKO, R. – VETROVII, A. – PIK, A. 2012. Improving the technical level of flexible screw conveyors. Monograph, Ternopol : Vektor, 202 pp. (In Ukrainian: Povyshenie technicheskogo urovnja gibkich vintivych konveijerov).

HEVKO, R. – ROZUM, R. – KLENDIY, O. 2016. Development of design and investigation of operation processes of loading pipes of screw conveyors. In INMATEH – Agricultural Engineering, vol. 50, no. 3, pp. 89–96.

HEVKO, R. – VITROVYI, A. – KLENDII, O. – LIUBEZNA, I. 2017. Design engineering and substantiation of the parameters of sectional tools of flexible screw conveyers. In Bulletin of the Transilvania University of Brasov, vol. 10, no. 59, pp. 39–46.

HEVKO, R. – ZALUTSKYI, S. – HLADYO, Y. – TKACHENKO, I. – LYASHUK, O. – PAVLOVA, O. – POHRISHCHUK, B. – TROKHANIAK, O. – DOBIZHA, N. 2019. Determination of interaction parameters and grain material flow motion on screw conveyor elastic section surface. In INMATEH – Agricultural Engineering, vol. 57, no. 1, pp. 123–134.

LECH, M. 2001. Mass flow rate measurement in vertical pneumatic conveying of solid. In Powder Technology, vol. 114, no. 1–3, pp. 55–58.

LOVEIKIN, V. – ROGATYNSKA, L. 2011. A model of loose material transportation by means of high speed conveyers with elastic operating devices. In Bulletin of Termopil Ivan Puluj National Technical University, vol. 16, pp. 66–70. (In Ukrainian: Model transportuvannja sipkogo vantazhu shvidkohodnimim gvintovimi konveerami z elastichnymi rabochimi organami).

LYASHUK, O. – ROGATYNSKA, O. – SERILKO, D. 2015. Modeling of the vertical screw conveyer loading. In INMATEH – Agricultural Engineering, vol. 45, no. 1, pp. 87–94.

MONDAL D. – GHOSH, N. 2018. Study on filling factor of short length screw conveyor with flood-feeding condition. In Materials Today: Proceedings, vol. 5, pp. 1286–1291.

OWEN, P. J. – CLEARY, P. W. 2010. Screw conveyor performance: comparison of discrete element modelling with laboratory experiments. In Progress in Computational Fluid Dynamics, vol. 10, no. 5–6, pp. 327–333.

PANKIV, V. – TOKARCHUK, O. 2017. Investigation of constructive geometrical and filling coefficients of combined grinding screw conveyor. In INMATEH – Agricultural Engineering, vol. 51, no. 1, pp. 59–68.

QI, J. – MENG, H. – KAN, Z. – LI, C. – LI, Y. 2017. Analysis and test of feeding performance of dual-spiral cow feeding device based on EDEM. In Transactions of the Chinese Society of Agricultural Engineering, vol. 33, no. 24, pp. 65–71.

ROBERTS, A. W. 2015. Bulk solids: optimizing screw conveyors. In Chemical Engineering, vol. 122, no. 2, pp. 62–67.

ROHATYNSKYI, R. – DIACHUN, A. – VARIAN, A. 2016. Investigation of kinematics of grain material in a screw conveyor with a rotating casing. In Bulletin of Kharkiv Petro Vasylenko National Technical University of Agriculture, no. 168, pp. 24–31.

TIAN, Y. – YUAN, P. – YANG, F. – GU, J. – CHEN, M. – TANG, J. – SU, Y. – DING, T. – ZHANG, K. – CHENG, Q. 2018. Research on the principle of a new flexible screw conveyor and its power consumption. In Applied Sciences, vol. 8, no. 7, article no. 1038.

UA 85011: 2013. Ukrainian patent. Sectional spiral.

YAO, Y. P. – KOU, Z. M. – MENG, W. J. – HAN, G. 2014. Overall performance evaluation of tubular scraper conveyors using a TOPSIS-based multiattribute decision-making method. In Scientific World Journal, vol. 2014, article no. 753080.